KONA Powder and Particle Journal No. 40 (2023) 219–235/https://doi.org/10.14356/kona.2023008 Original Research Paper

Computational Fluid Dynamic Modelling of Fully-Suspended Slurry Flows in Horizontal Pipes with Different Solids Concentrations †

Gianandrea Vittorio Messa [1]*, Qi Yang [1], Maria Graça Rasteiro [2], Pedro Faia [3], Vaclav Matoušek [4], Rui C. Silva [2] and Fernando Garcia [2]

[1] *Department of Civil and Environmental Engineering, Politecnico di Milano, Italy*
[2] *Chemical Process Engineering and Forest Products Research Centre, Department of Chemical Engineering, University of Coimbra, Portugal*
[3] *Center of Mechanical Engineering, Materials and Processes, Electrical and Computer Engineering Department, University of Coimbra, Portugal*
[4] *Department of Hydraulics and Hydrology, Faculty of Civil Engineering, Czech Technical University in Prague, Czech Republic*

Abstract

This research work is a significant step toward further understanding of the β-σ two-fluid model for the simulation of fully-suspended slurry flows in pipeline systems, with the goal of enhancing its potential for scientific research and engineering applications. Particularly, the focus of the study is the characterization and handling of the two main empirical coefficients of the model, namely, β and σ, which require case-specific tuning based on a given set of experimental data. Reference is made to the relevant case of slurry transport in horizontal pipes with infinite length. The influence of β and σ on different features of the fluid dynamic solution has been extensively investigated, considering also the role played by the specific testing conditions. Based on these findings, a procedure for determining appropriate values of β and σ has been developed, which requires only two experimental measurements, namely the concentration profile from a test at moderate slurry concentration, and the hydraulic gradient from another test in which the same slurry flows at high concentration. The procedure has been satisfactorily tested against published experimental data on pipe transport of fine glass bead and sand slurry.

Keywords: Computational Fluid Dynamics, slurry pipelines, hydro-transport, two-fluid modelling, model calibration

1. Introduction

Pipeline transport of solid particles in the form of slurry is frequently encountered in several engineering fields, such as mining, chemical, oil and gas, pharmaceutical, food, among others. In addition, understanding the physical mechanisms and the complex phenomena occurring in a slurry pipe is an extremely challenging task, as well is the development of mathematical models for their description. Therefore, it is not surprising to see that slurry pipe flows have been driving the efforts of researchers for several decades.

From a technical point of view, there are a few relevant parameters which characterize slurry pipe flows. Probably the key role is played by the hydraulic gradient, i_m (pressure drop in meters of water per pipe unit length), which quantifies the energy dissipation produced by the flow, and, thus, dictates the selection of the pump capacity. The hydraulic gradient for a certain solid volumetric concentration, C_{vi}, is often expressed as a function of the average slurry velocity, V_m, estimated by the ratio between the volumetric flow rate of the mixture, Q_m, and the pipe cross section area, A. When plotted, the trend of i_m versus V_m, for a certain C_{vi}, is called pipe characteristic curve. Actually, two types of concentrations can be defined for slurry pipe flows: one is the already mentioned C_{vi}, or in-situ concentration, which is the ratio between the volume of solids and the volume of slurry in a certain part of the system; the other is the delivered concentration, C_{vd}, which is the ratio between the volumetric flow rate of the solids, Q_s, and that of the mixture, Q_m. Finally, another important parameter is the deposition limit velocity, V_{dl}, which is the threshold value of average slurry velocity at which solids deposition starts to be observed.

The values of the just mentioned technical features and parameters, as well their relations, are strongly related with the internal structure of the flow. This has been usually quantified through several flow regimes, whose names and definitions are different in the literature. In this study, reference will be made to the well-established classification reported in the textbook of Wilson et al. (2006).

† Received 31 January 2022; Accepted 17 March 2022
J-STAGE Advance published online 4 June 2022
* Corresponding author: Gianandrea Vittorio Messa;
Add: 20133 Milano, Italy
E-mail: gianandreavittorio.messa@polimi.it
TEL: +39-02-2399-6287

Copyright © 2023 The Authors. Published by Hosokawa Powder Technology Foundation. This is an open access article under the CC BY license (https://creativecommons.org/licenses/by/4.0/).

Homogeneous flow (**Fig. 1a**) is typically composed by very fine solids, smaller than say 40 microns, flowing at high velocity. In this regime, the distribution of particles is virtually uniform along the flow. The (Reynolds-averaged) velocity is axisymmetric across the pipe cross section and there is no local slip between particles and carrying fluid velocities. Slurries with particles in the range between 200 microns and up to 1.5 % of the pipe diameter show a heterogeneous behavior (**Fig. 1c**). In this regime, the particles tend to get separated from the carrying liquid. This produces greater non-uniformity of the distributions of the solids concentration and velocity, especially at low velocities. In the case of coarse sands and fine gravel (size bigger than say 800 microns), heterogeneous flow becomes more distinctly stratified with a detectable sliding bed. Finally, fully stratified flow occurs when large and rapidly settling particles travel in the lower part of the pipe by ether saltation or as a moving bed (**Fig. 1e**). Threshold conditions occur between the three main flow patterns described above. These are the pseudo-homogeneous regime (**Fig. 1b**), in-between the homogeneous and the heterogeneous ones, and the partially stratified regime (**Fig. 1d**), in-between the heterogeneous and the fully stratified ones. The pseudo-homogeneous regime is the focus of the present work. This pattern takes place when particles in the range in between 40 to 200 micron (typically fine sand) flow at relatively high velocities, and it is characterized by a moderate, yet clearly detectable, vertical concentration gradient and a slightly asymmetrical velocity profile.

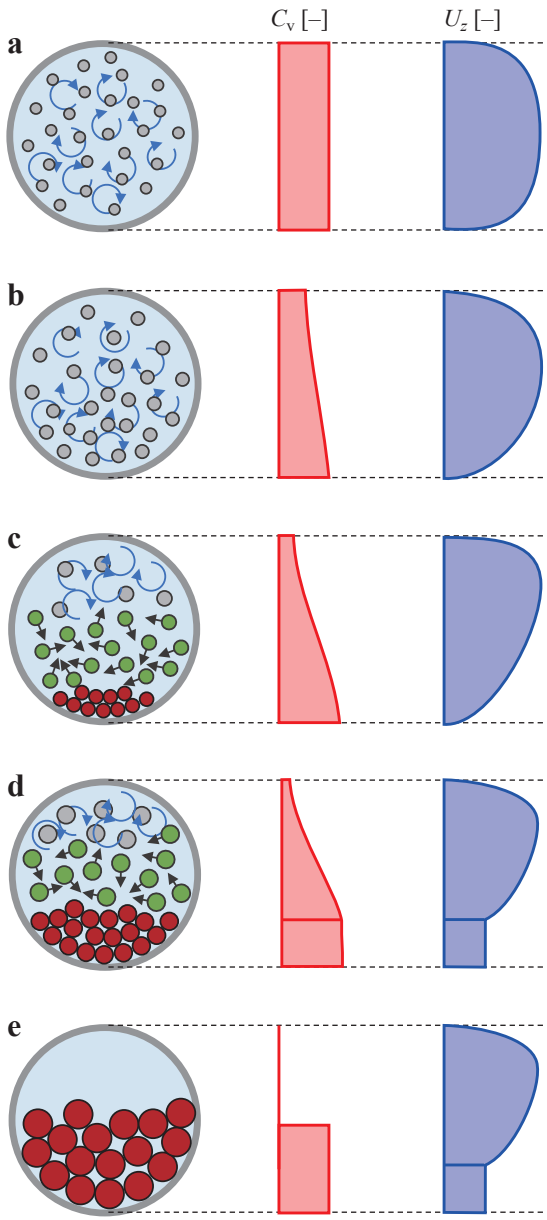

Fig. 1 Main flow regimes of slurry pipe flow: **(a)** homogeneous flow; **(b)** pseudo-homogeneous flow; **(c)** heterogeneous flow; **(d)** partially stratified flow; **(e)** fully stratified flow. The sketches denoted by C_v and U_z indicate the typical solid volume fraction and Reynolds-averaged fluid velocity profiles along the vertical diameter. In the sketches on the left, the color of the particles indicates the key mechanism driving the flow: grey = particle–fluid interactions; green = quick particle–particle collisions; red = enduring particle–particle contacts.

Several sorts of models have been developed for the prediction of slurry parameters. Traditionally, they fit in two main categories. The first includes models based on integral (cross-section averaged) quantities which produce empirical or semi-empirical correlations for relevant parameters such as i_m or V_{dl}, as was done by Durand (1953) and Thomas (1979). The second category is that of mechanism-based layered models: Wilson (1976) developed one, starting from a simplified description of the inner structure of the flow.

Indeed, empirical and mechanistic models have been and still are a powerful tool for slurry pipeline design and management, as well as for researchers. At the same time, an intrinsic limitation is that, despite taking the basic transport mechanisms into account, these models are not able to characterize them at the local level. This does not allow deep insight into the flow, nor exploring geometries and flow conditions different from those considered for the calibration of the model coefficients and parameters. Numerical simulations based on Computational Fluid Dynamics (CFD) might allow overcoming such limits, since CFD modelling is inherently local and distributed. As discussed in Messa et al. (2021b), the CFD approach requires switching from a macroscopic description of the flow, i.e. the flow regimes in **Fig. 1**, on which traditional slurry models are based, to a particle-scale description based on the key physical mechanisms driving the flow at the local level. These are interaction between the particles and the turbulent fluid, quick particle–particle collisions, and long-lasting inter-granular contacts. As it is indicated by the color of the particles in **Fig. 1**, homogeneous and pseudo-homogeneous flow are driven by particle–fluid interactions, whereas fully stratified flow is contact-dominated. Conversely, all the three basic mechanisms play a role in heterogeneous and partially stratified flow.

There is no doubt that CFD has great potential as a tool for investigating slurry pipe flows. The local nature of a CFD model, in fact, opens up the possibility of (virtually) investigating geometries with no constraints in size and complexity, providing much more information when compared to laboratory testing. At the same time, this approach is also not free from criticisms. Depending on the modelling approach and type of flow, CFD simulations might require large computational costs, which could become practically unaffordable. For instance, describing particle–particle interactions in the Lagrangian framework is not currently feasible for the typical concentrations of slurry pipelines, making Eulerian-based methods (i.e. two-fluid model and mixture model) the preferred or even the only viable route for engineering computations. Apart from that, it must be noted that all CFD models for slurry flows are approximated in nature, and they include several closure parameters, and coefficients which, practically speaking, cannot be decided based on other criteria than the fitting of experimental data for certain conditions. This means that, in the end, CFD modelling cannot dismiss laboratory (or field) testing, but the two approaches should act in a synergistic way. And that is where the main challenges of CFD modelling arise, especially but not exclusively, in the context of its application to slurry pipelines.

As pointed out in Messa et al. (2021b), CFD modelling might have different scopes and impact. On the one hand, interpretative models are calibrated for specific flow conditions and then used to infer local and difficult-to-measure features of the flow under the same testing conditions only. This is the case, for instance, of a model whose calibration procedure uses a set of hydraulic gradient and concentration profile measurements, employed to gather information on the particle velocity distribution for the same experimental conditions. On the other hand, predictive models allow predicting one or more features of the flow outside the calibration conditions. Interpretative models are suitable for achieving a comprehensive and detailed picture of the flow overcoming the limitations of experiments; thus, they are very useful in research, in advanced design, and in the management of existing systems. Conversely, predictive models can be a fundamental tool for the design of new systems.

Although scientific research on the CFD usage in modelling of slurry pipe flows dates back to the 1980s, with an impressive increase in the number of published papers during the last 5–10 years, there is still a long way to go in the exploitation of its potential of application in this field. Among the most significant studies in the field, those authored by Roco and Shook (1983), Ling et al. (2003), Ekambara et al. (2009), Kaushal et al. (2012), Capecelatro and Desjardins (2013), Messa et al. (2014), Uzi and Levy (2018), Messa and Matoušek (2020) shall be mentioned. The interested reader is referred to Messa et al. (2021b) for a comprehensive review of the state-of-the-art in the field. The aforementioned review paper concluded that most of the existing models might be regarded as interpretative, even if some works do not meet the proper verification and validation requirements, being the initial code verification stage via convergence testing one of them. For sure, very few models proved or even looked predictive in the sense previously introduced. This is not surprising, because the demonstration of the predictive capacity of a model requires going well beyond its evaluation with the existing experimental database, but also the extrapolation to new sets of conditions. Two different procedures have been followed in previous studies. The former consists of calibrating the model by referring only to a subset of the experimental database, while employing the remaining sets of data for validation. An attempt is this sense was reported, for instance, in Messa and Matoušek (2020). The second and different strategy was adopted in Ekambara et al. (2009) and Messa et al. (2014), and consists of the verification that the same combination of calibration coefficients allows for a reasonably good agreement with the largest possible experimental data available in the measurements database, which basically means that calibration and validation are no longer two distinct phases.

For about ten years, research work has been carried out at Politecnico di Milano on the development of CFD models for the simulation of slurry pipe flows. The main outcome of this research, achieved with important contributions from Concentration, Heat, and Momentum Limited (CHAM Ltd, London) and from Institute of Hydrodynamics of the Czech Academy of Sciences, is the already mentioned β-σ two-fluid model. Whereas the first efforts were devoted to the definition of the model formulation (Messa and Malavasi, 2015), recently the focus has been directed mostly to the assessment of the predictive capacity of the model.

The research work illustrated in the present paper fits into this trend and represents an important step towards the usability increase of the two-fluid model in an industrial context. The role played by the two main tuning coefficients of the model, β and σ, has been established through an extensive sensitivity analysis. The goal was to understand which features of the CFD solution are mostly affected by β and σ, taking into account also the physical conditions of the simulated problem (pipe diameter, bulk velocity, in-situ concentration, etc.), in order to develop an appropriate procedure for calibration of the two parameters.

The remaining of the paper is divided into three sections, followed by the conclusions. In **Section 2**, the main features of the β-σ two-fluid model and of the CFD setup are briefly illustrated. In **Section 3**, the results of the sensitivity analysis are presented, and the procedure for calibrating β and σ is proposed. Finally, in **Section 4**, three examples of application of the calibration strategy are presented

and discussed, referring to glass bead and fine sand slurry experimental data reported in the literature.

2. Mathematical model

2.1 Overview of the β-σ two-fluid model

The β-σ two-fluid model is an extension of the IPSA (Inter-Phase Slip Algorithm) of Spalding (CHAM, 1994a) for turbulent slurry flow. Being a two-fluid model, it is based on the Eulerian-Eulerian approach, in which both phases are interpreted as interpenetrating continua and solved in the Eulerian, cell-based framework. The reader is referred to Messa and Matoušek (2020) for the complete set of conservation equations and closures. Only the essential features are summarized here.

The fundamental conservation equations of the β-σ two-fluid model are for the mass and momentum of the two phases. Under steady-state conditions, the ones considered in this study, their formulation is as follows:

$$\nabla \cdot \Phi_l \rho_l \boldsymbol{U} = \nabla \cdot \left(\frac{\mu_l^t}{\sigma} \nabla \Phi_l \right) \tag{1}$$

$$\nabla \cdot \Phi_s \rho_s \boldsymbol{V} = \nabla \cdot \left(\frac{\mu_s^t}{\sigma} \nabla \Phi_s \right) \tag{2}$$

$$\nabla \cdot \Phi_l \rho_l \boldsymbol{U}\boldsymbol{U} = -\Phi_l \nabla P + \nabla \cdot \Phi_l \left(\mu_l + \mu_l^t \right) \nabla \boldsymbol{U} + \Phi_l \rho_l \boldsymbol{g} + \boldsymbol{M}_l + \nabla \cdot \left(\frac{\mu_l^t}{\sigma} \boldsymbol{U} \nabla \Phi_l \right) \tag{3}$$

$$\nabla \cdot \Phi_s \rho_s \boldsymbol{V}\boldsymbol{V} = -\Phi_s \nabla P + \nabla \cdot \Phi_s \left(\mu_s + \mu_s^t \right) \nabla \boldsymbol{V} + \Phi_s \rho_s \boldsymbol{g} + \boldsymbol{M}_s + \nabla \cdot \left(\frac{\mu_s^t}{\sigma} \boldsymbol{V} \nabla \Phi_s \right) \tag{4}$$

where: Φ_l, $\boldsymbol{U}$, μ_l, and μ_l^t are the locally averaged volume fraction, the locally averaged velocity vector, the viscosity, and the eddy viscosity of the liquid phase, respectively; Φ_s, $\boldsymbol{V}$, μ_s, and μ_s^t are the corresponding variables for the solid phase; P is the locally averaged pressure, shared by the phases; $\boldsymbol{g}$ is the gravitational acceleration vector; and $\boldsymbol{M}_l$ and $\boldsymbol{M}_s$ are the generalized drag term, which will be discussed later. Clearly, Φ_l and Φ_s sum up to a unit value.

A key feature of the β-σ two-fluid model, inherited from the original IPSA, is the presence of phase diffusion terms, which are the last terms on the right-hand side in Eqns. (1–4). The origin of these terms has been discussed in Messa et al. (2021b) on the grounds of the previous derivations of Burns et al. (2004): they basically arise from the modelling of the correlations between the fluctuating velocities and the fluctuating volume fractions, and they account for the effect of particle turbulent dispersion. The coefficient, σ, used to calculate the diffusion coefficient of the phase diffusion terms, is called turbulent Schmidt number for volume fractions, and it is one of the two main calibration parameters of the β-σ two-fluid model.

The second calibration coefficient, β, appears in the evaluation of the friction parameter $\tilde{\mu}_m$, which is expressed as a function of the volume fraction of the solid phase, through the following empirical correlation,

$$\tilde{\mu}_m = \mu_l \exp\left\{ \frac{2.5}{\beta} \left[\frac{1}{(1-\Phi_s)^{\beta}} - 1 \right] \right\} \tag{5}$$

built and based on the formal analogy with the correlation of Cheng and Law (2003) for the viscosity of the mixture of colloidal suspensions. Although $\tilde{\mu}_m$ (and, thus, also β) does not appear explicitly in Eqns. (1–4), it comes into play twice in the β-σ two-fluid model. Firstly, it is used to evaluate the viscosity of the solid phase, μ_s, assuming that μ_l, μ_s, and $\tilde{\mu}_m$ are related with each other through the following equation

$$\tilde{\mu}_m = \mu_l \Phi_l + \mu_s \Phi_s \tag{6}$$

The solid phase viscosity μ_s, in turn, appears both in the momentum equation for that phase (Eqn. (4)) and in the wall boundary condition for the solid phase, which will be briefly illustrated later in **Section 2.3**. In addition to the evaluation of μ_s, $\tilde{\mu}_m$ is used to calculate the generalized drag terms, $\boldsymbol{M}_l$ and $\boldsymbol{M}_s$. These two terms account for the exchange of momentum between the two phases within each local control volume, and, considering the action-reaction principle, they are equal in intensity and opposite in sign. In the β-σ two-fluid model, it is assumed that the inter-phase momentum exchange is uniquely due to the drag force, and so $\boldsymbol{M}_l$ and $\boldsymbol{M}_s$ are given by

$$\boldsymbol{M}_s = -\boldsymbol{M}_l = \frac{3}{4 d_p} \Phi_s \rho_l C_d \left| \boldsymbol{U} - \boldsymbol{V} \right| (\boldsymbol{U} - \boldsymbol{V}) \tag{7}$$

where d_p is the volume-equivalent particle diameter, and C_d is the drag coefficient. As in many two-fluid models, C_d is obtained through the Schiller and Naumann (1935) correlation for a single spherical particle. However, a distinguishing feature in the β-σ model resides in the fact that the input of the Schiller and Naumann's correlation is not the usual particle Reynolds number, but a modified Reynolds number based on ρ_l, d_p, $|\boldsymbol{U}\text{-}\boldsymbol{V}|$, and on the friction parameter $\tilde{\mu}_m$. The rationale behind this definition is the need to account for the increased flow resistance encountered by a single particle at high local solid concentration. Additionally, it is a simple way to account for the effect of particle shape through the empirical parameter β.

The eddy viscosities, μ_l^t and μ_s^t, are obtained from two-phase turbulence models. Particularly, μ_l^t is calculated through the two-phase extension of the k-ε standard turbulence model for high Reynolds number flows, which is embedded in the PHOENICS code (CHAM, 1994b). Thus, μ_l^t is obtained through the solution of two partial differential equations for the turbulent kinetic energy per unit mass of the carrier fluid, k_l, and its dissipation rate per unit mass, ε_l. Conversely, μ_s^t is directly obtained from μ_l^t through the following algebraic constraint

$$\frac{\mu_l^t}{\rho_l} = \frac{\mu_s^t}{\rho_s} \tag{8}$$

2.2 Applicability conditions

The applicability conditions of the β-σ two-fluid model have been individuated in Messa and Matoušek (2020). The first comes from the wall boundary condition of the solid phase, and it imposes that:

$$d_p^{+B} = \frac{d_p}{\frac{\mu_l}{\rho_l V_m}\left[0.039\left(\frac{\rho_l V_m D}{\mu_l}\right)^{-0.25}\right]^{-0.5}} < 30 \tag{9}$$

where d_p^{+B} is the ratio between d_p and the viscous length scale estimated using the Blasius correlation for the coefficient of frictional resistance of turbulent single–phase flows in smooth straight pipes (Schlichting, 1979), and D is the pipe diameter. The two other constraints quantify the condition in which the flow must be dominated by particle turbulent interactions, without any role being played by particle–particle interactions. In Messa and Matoušek (2020), such condition has not been related to any of the flow regimes in **Fig. 1**, but it was referred to as "fully suspended flow". However, it could be reasonably claimed that the flow regime in which the β-σ two-fluid model is applicable, is the pseudo-homogeneous one (**Fig. 1b**). Mathematically speaking, the two constraints are:

$$V_m = 1.5 V_{dl}^T \tag{10}$$

$$\Phi_s < 0.45 \tag{11}$$

where V_{dl}^T is the estimate of the deposition limit velocity obtained from the correlation of Thomas (2015).

2.3 CFD setup

The computational domain and the boundary conditions imposed are the same as in Messa and Matoušek (2020), namely, a cylindrical volume 120D long, bounded by an inlet, an outlet, and a solid wall (**Fig. 2**).

At the inlet, uniform distributions have been imposed for the axial velocities of the two phases, $U_z^{in} = V_z^{in} = V_m$, for their volume fractions, $\Phi_s^{in} = 1 - \Phi_l^{in} = C_{vi}$, for the turbulent kinetic energy of the liquid, k_l^{in}, and for its dissipation rate, ε_l^{in}. The values of the last two parameters have been set based on a turbulence intensity of 0.05 and on a length scale of 0.07D, as explained in Messa and Matoušek (2020). At the outlet, the pressure is set to zero, as well as the normal gradient of all solved variables. At the walls, the shear stress of the liquid, τ_l^w, as well as the values of the turbulent parameters in the near-wall cells, k_l^w and ε_l^w, are obtained from the equilibrium wall function option, available in PHOENICS (CHAM, 1994c). Conversely, the wall shear stress of the solid phase on the surface of the near-wall cells, τ_s^w, was obtained through the following expression, implemented in PHOENICS through a user-defined function:

$$\tau_s^w = \Phi_s^w \rho_s s_s \left|\boldsymbol{V}^{\parallel}\right|^2 \tag{12}$$

where the $\boldsymbol{V}^{\parallel}$ is the resultant velocity of the solid phase parallel to the wall at the first grid node, Φ_s^w is the solid volume fraction in the near-wall cells, and s_s is the friction factor of the solid phase, given by the following implicit equation

$$s_s = \frac{\kappa^2}{\ln^2\left(E \cdot Re_s^w \sqrt{s_s}\right)} \tag{13}$$

where $\kappa = 0.41$ is the von Karman constant, E is a roughness parameter, set at 8.6 as recommended for smooth walls, and Re_s^w is a wall Reynolds number defined in terms of ρ_s, $\left|\boldsymbol{V}^{\parallel}\right|$, μ_s, and of the normal distance of the first grid point to the wall, δ (**Fig. 3a**). Since μ_s is obtained from μ_l^t (Eqn. (6)) which, in turn, is a function of β (Eqn. (5)), it is not surprising to see that this coefficient plays a role in the predictions of the frictional losses. Evidence of this claim will be given later.

In this study, the used code; PHOENICS version 2018 (CHAM, 2002) and all settings of the solution algorithm (FV formulation, differencing schemes, relaxation factors, convergence criteria, etc.) were the same as detailed in Messa and Matoušek (2020). Similarly, the grid was a structured one in cylindrical-polar coordinates, consisting of 30, 30, and 200 subdivisions along the azimuthal, radial, and axial directions, respectively (**Fig. 3b**). The azimuthal

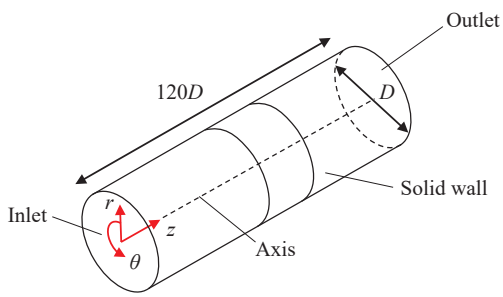

Fig. 2 Computational domain and boundary conditions.

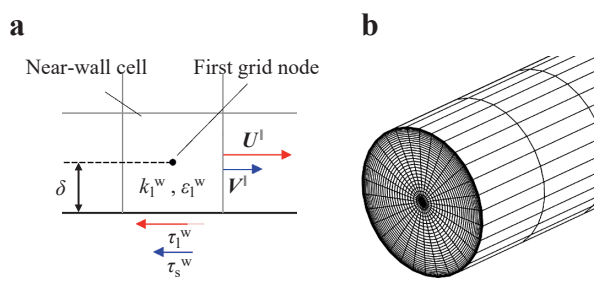

Fig. 3 Sketch of **(a)** a near wall cell and **(b)** of the computational mesh.

and axial subdivisions were uniform, whereas the radial ones were progressively reduced when moving away from the pipe axis. Thus, the smallest radial subdivisions were those adjacent to the pipe wall. On the grounds of the findings in Messa et al. (2021a), their size was set equal to 60 times the viscous length scale obtained by the Blasius correlation for turbulent single-phase flows in straight pipes. This implies that, although the total number of cells was the same for all simulations, their distribution over the pipe section was changed according to the inlet velocity, V_m. Note that, with the cylindrical-polar mesh, additional boundary conditions are needed along the pipe axis, which were of zero-flux type.

3. Analysis of the effects of β and σ on the key features of the CFD solution and development of a calibration strategy

Three necessary steps for proving that a model has a predictive capacity are (i) the identification of the calibration coefficients, (ii) the assessment of their role on the different features of the solution, and (iii) the development of a precise calibration strategy. The β-σ two-fluid model has two main calibration coefficients, β and σ. Note that the number of empirical parameters becomes much higher if one includes the numerical constants in the turbulence model. However, dealing with a large number of tuning coefficients would make the calibration difficult and the model less robust; therefore, the turbulence model constants were simply set with the default values for single-phase flow (Launder and Spalding, 1974), and the β-σ two-fluid model has been regarded as a two-parameter model.

Once the calibration parameters have been identified, their role in the different features of the CFD solution must be established. This requires not only to specify the range of variability of β and σ and to select the features of the solution of most interest, but also to define the physical conditions for the sensitivity analysis. In fact, β and σ might play different roles depending on the specific characteristics of the slurry flow subject of investigation, i.e. for different levels of concentration, pipe diameter, bulk mean velocity etc. Starting from this last task, it could be observed that the physical conditions characterizing a slurry pipe flow are defined by the pipe diameter, D, the pipe roughness, the slurry velocity V_m, the in-situ concentration C_{vi}, the particle properties, and the properties of the carrier fluid. In principle, the sensitivity analysis upon β and σ should be carried out within a suitable range of all the physical features above mentioned, and, for each physical condition, different values of β and σ should be considered. However, this would result in an unnecessarily large number of simulations and, therefore, some simplifications were made. Firstly, the pipe walls were considered hydraulically smooth, thereby neglecting the pipe roughness. The choice was made because, in its original formulation, the β-σ two-fluid model is unable to account for pipe roughness. Indeed, a rough wall function option is available in PHOENICS for the liquid phase, but no study has been made for the solid phase. Additionally, the pipe roughness in the experiments used for calibrating and validating the β-σ two-fluid model was generally very low (Kaushal and Tomita, 2007; Matoušek, 2002; Schaan et al., 2000). Secondly, also the particle properties, particle size and particle density were kept fixed in the sensitivity analysis, on the grounds of the following considerations. On one hand, typical materials used in slurry pipe flow experiments include glass beads and natural sand, whose densities are rather close to each other. On the other hand, preliminary simulations run at the beginning of this research work indicated that the role played by β and σ is substantially unaffected by the value of particle diameter within the typical range where this model applies, say 100 μm to 200 μm. Based on the above, the sensitivity analysis was performed considering particles with density of 2650 kg/m^3 and size of 150 μm. Particle shape is very different for glass bead and sand, and also among sand grains. However, particle shape is not set a priori in the β-σ model, but only indirectly through the empirical parameters β and σ.

Finally, also the properties of the carrier liquid have not been varied (density, viscosity, rheological model) but the characteristic features of water have been taken, namely $\rho_l = 998.23$ kg/m^3, $\mu_l = 0.001$ Pa·s, and Newtonian rheology. It is expected that reasonably small variations in terms of ρ_l and μ_l will not alter the conclusions of the sensitivity analysis. The study of the effect of the rheological model will be addressed in future research, as it will require developing a non-Newtonian formulation of the β-σ two-fluid model, currently unavailable.

Based on the considerations above, in the selection of the physical conditions of the sensitivity analysis, reference was made only to the pipe diameter, D, to the slurry velocity, V_m, and to the in-situ concentration, C_{vi}. For each of the three parameters, two "extreme" values have been considered to span the broadest possible range of applicability of the β-σ two-fluid model, defined by the three applicability constraints in **Section 2.2**. In particular, the pipe diameter was either 50 mm ("small" pipe) or 500 mm ("large" pipe); the bulk velocity was either 2 m/s ("low" velocity) and 4.5 m/s ("high" velocity); the in-situ concentration was either 0.05 ("low" concentration) or 0.40 ("high" concentration). Only the "high" velocity was considered in the large pipe runs, as the 2 m/s value does not fulfil the constraint $V_m = 1.5V_{dl}^T$ (Eqn. (10)). Thus, the total number of combinations was equal to six, as summarized in **Table 1**. For each of the six aforementioned scenarios, different combinations of β and σ were considered. Particularly, σ was either 0.50, 0.75, or 1.00, whereas β was either 0.50, 1.50, 2.50, or 3.50. The effects of varying σ were studied for $\beta = 2.50$, whereas that of varying β was investigated for $\sigma = 0.75$.

The target variables of the sensitivity analyses were those of most interest in slurry pipeline systems, namely, the hydraulic gradient, i_m, the chord-average volume fraction profile, the vertical profile of the locally-averaged fluid velocity, and the distributions of the wall shear stresses of the two phases over the pipe circumferences. Note that the vertical profile of the locally-averaged velocity of the solid phase has not been investigated, as the axial slip between the two phases was very small for all simulated cases, as typical of the pseudo-homogeneous regime.

Due to space limitations, only the most significant results will be provided in the form of tables and figures, but all of them are available upon request to the corresponding author. **Table 2** summarizes the values of hydraulic gradient, i_m, as obtained for all the combinations of β and σ and all testing conditions in **Table 1**. The results highlight that the effect of σ on i_m is negligible or even lacking, whereas β affects i_m but only at high concentration (cases C3, C4, C6). More generally, the effect of β at low concentration was found to be negligible not only in terms of hydraulic gradient, but also in terms of all other features of the flow under investigation, namely, concentration profile, velocity profile and wall shear stresses distributions. This is not surprising, if one considers that β plays a role in the model through its appearance in the formula for the friction parameter $\tilde{\mu}_m$ (Eqn. (5)) and, according to the mathematical formulation employed, the effect of β on $\tilde{\mu}_m$ is very limited at low Φ_s.

For all levels of concentration, the predicted concentration profiles are affected by the value of σ, as shown in **Fig. 4b**, **d** for the two exemplary cases C1 and C6. Increasing σ will increase the vertical concentration gradient, which is a clear consequence of the phase diffusion terms in the mass conservation equations (Eqns. (1) and (2)). As already mentioned, no effect of β can be detected at low concentration, as shown in **Fig. 4a** for case C1. Conversely, β was found to significantly affect the concentration profile at high concentration, as seen in **Fig. 4c** for case C6.

The predicted velocity profiles appear substantially insensitive to the values of β and σ for all the testing conditions. The greatest effect is observed when varying β at high concentration, but the change in the velocity values is still rather moderate (**Fig. 5**).

The wall shear stresses of the two phases are, in general, affected by both β and σ. At high concentration, an obvious increase in τ_s^w is evident for increasing β (**Fig. 6a**), which is the direct consequence of the higher friction factor s_s produced by a higher wall Reynolds number Re_s^w (Eqn. (13)). At both low and high concentration, varying σ will modify the individual distributions of τ_l^w and τ_s^w (**Figs. 6b, c**). However, comparing the curves in **Figs. 6b**, **c** with the corresponding volume fraction profiles (shown in **Fig. 4b** for case C6 at $\beta = 2.5$ only) suggests that the variations in τ_l^w and τ_s^w mainly arise from the effect of σ on the volume fraction in the near-wall cells rather than from a direct influence of σ on the friction factors of the two phases. It is interesting to note that, although σ has an effect on the individual wall shear stresses distribution, this parameter was found to have practically no influence on the hydraulic gradient (**Table 2**), which is related with the average value of their sum:

Table 1 Simulation scenarios in the sensitivity analysis. The other physical parameters were $\rho_l = 998.23$ kg/m³, $\mu_l = 0.001$ Pa·s, $\rho_s = 2650$ kg/m³, $d_p = 150$ µm.

Case ID	D [mm]	V_m [m/s]	C_{vi} [-]
C1	50	2	0.05
C2	50	4.5	0.05
C3	50	2	0.40
C4	50	4.5	0.40
C5	500	4.5	0.05
C6	500	4.5	0.40

Table 2 Effect of β and σ on the predicted hydraulic gradient for the six testing conditions in **Table 1**.

Model parameters							
β	2.5			0.50	1.50	2.50	3.50
σ	0.50	0.75	1.00	0.75			
i_m [-]							
C1	0.079	0.080	0.082	0.080	0.080	0.080	0.081
C2	0.331	0.333	0.335	0.332	0.332	0.333	0.333
C3	0.198	0.199	0.199	0.144	0.162	0.199	0.293
C4	0.825	0.825	0.825	0.607	0.680	0.825	1.203
C5	0.023	0.023	0.023	0.023	0.023	0.023	0.023
C6	0.051	0.051	0.051	0.040	0.044	0.051	0.071

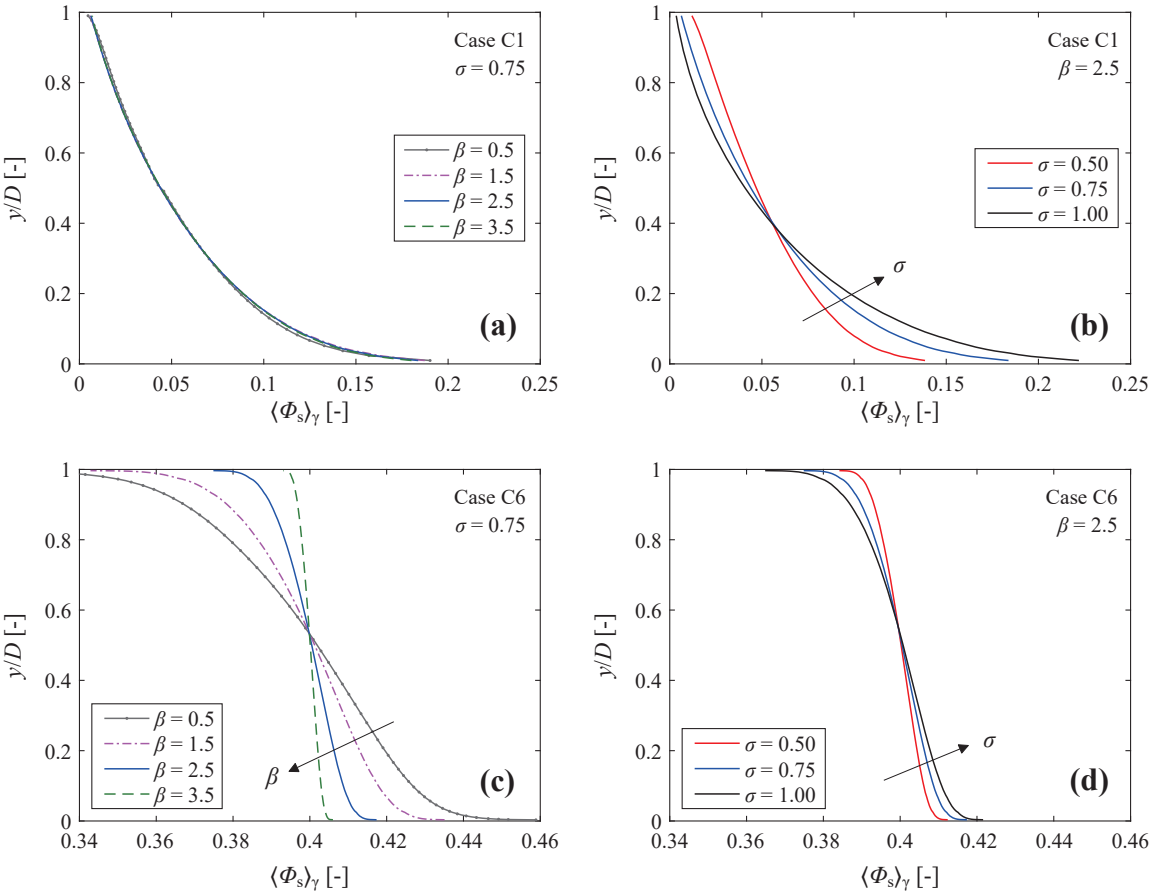

Fig. 4 Effect of β and σ on the predicted chord-averaged concentration profile for cases C1 and C6.

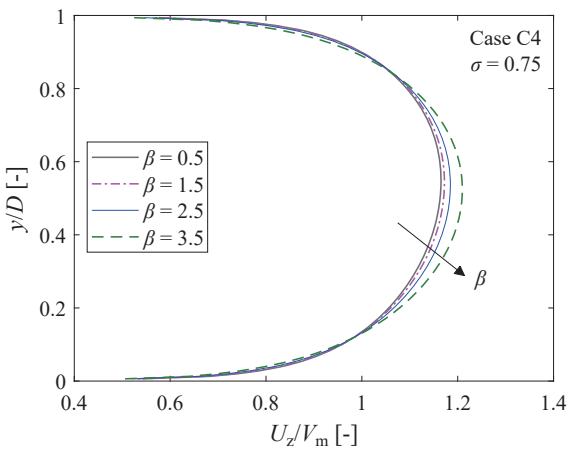

Fig. 5 Effect of β on the predicted fluid velocity profile for case C4.

$$\rho_l |\boldsymbol{g}| i_m \left(\pi \frac{D^2}{4}\right) = \frac{D}{2} \int_0^{2\pi} \left(\tau_l^w + \tau_s^w\right) d\theta \tag{14}$$

Based on the results of the sensitivity analysis, a strategy was proposed for the calibration of the two parameters β and σ. The strategy is arranged into two steps in sequence. Firstly, in a first-attempt, β is chosen and an appropriate σ is determined by referring to the concentration profile data at low concentration. Secondly, using this value of σ, a more appropriate β is found by referring to the hydraulic gradient data at high concentration. Therefore, in order to calibrate β and σ, one needs at least one experimentally determined concentration profile at low concentration (say 10 %) and one measured value of hydraulic gradient at high concentration (say 30–40 %). In the two calibration tests, the same type of particles shall be used, but no specific constraints are given in terms of mixture velocity and pipe diameter, provided that the three applicability conditions of the β-σ model are fulfilled. As it will be demonstrated in **Section 4**, the two calibration tests might have different V_m. In principle, the pair of values of β and σ obtained from this calibration procedure should allow for reasonably accurate prediction over the entire range of C_{vi} spanned by the two calibration tests, and that they are also appropriate over the entire range of V_m determined by the two conditions defined by Eqns. (9) and (10) (which does not depend on the C_{vi}).

The rationale behind the proposed strategy is the solution of the β-σ two-fluid model is practically insensitive to the value of β for low concentration cases, as shown in **Table 2** (cases C1, C2, C5) and **Figs. 4a** and **6a**, whilst, for high concentration cases, the hydraulic gradient is not affected by σ but only by β (**Table 2**, cases C3, C4, C6). However, for the same high concentration cases, β does not influence only the hydraulic gradient, but also the concentration

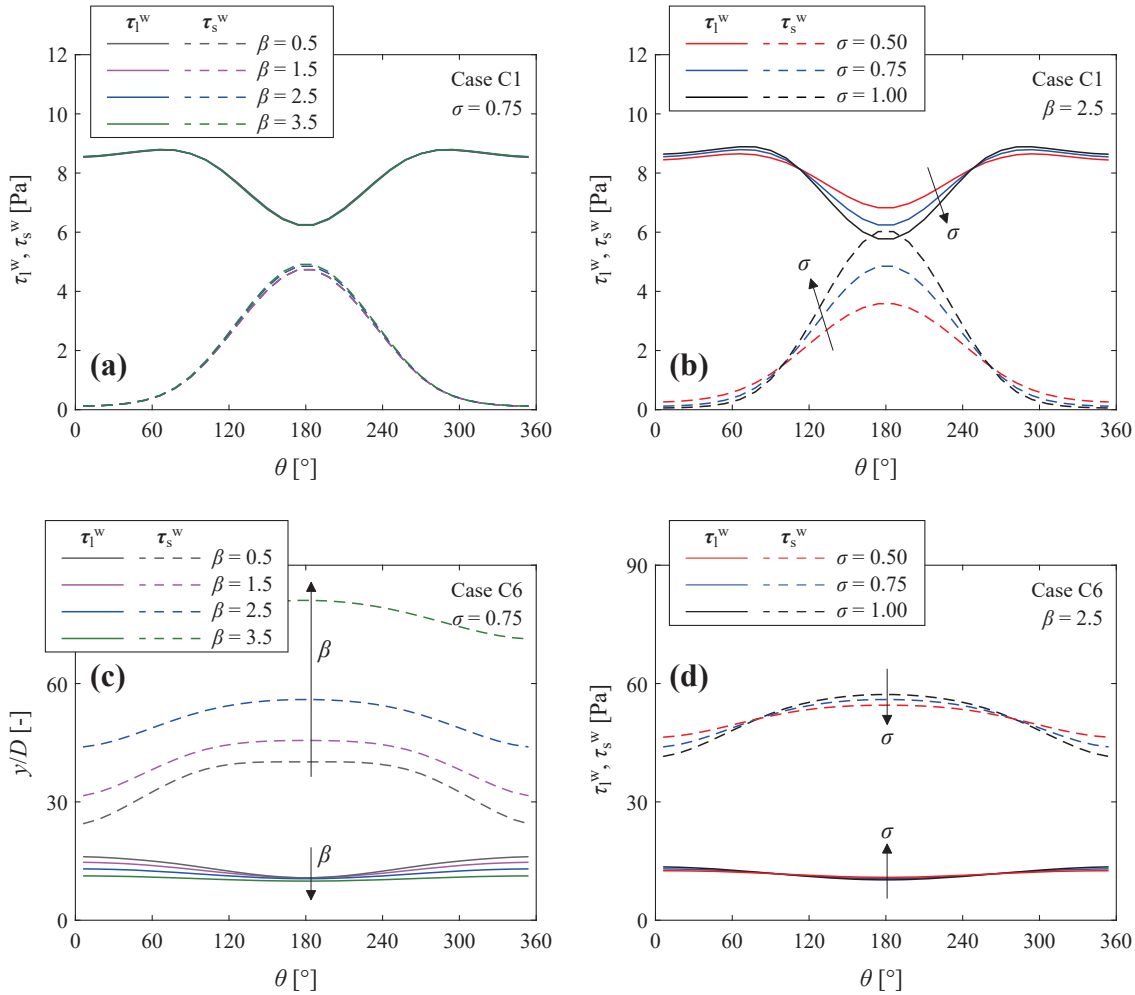

Fig. 6 Effect of β and σ on the predicted distributions of the wall shear stresses of the two phases for cases C1 and C6. According to the coordinate system in **Fig. 1**, $\theta = 0$ and $\theta = 180°$ indicate the crown and the invert of the pipe, respectively.

profile (**Fig. 4c**). Therefore, the effects of σ and β cannot be fully decoupled, as requested by the proposed calibration methodology; as a result, deviations might be expected for high concentration cases in terms of concentration profile. Strengths and weaknesses of the calibration strategy, and of the β-σ formulation from a more general perspective, will be discussed in the next section. Three verification tests will be presented, employing experimental data reported in the literature.

4. Verification of the calibration strategy against experimental data

4.1 Experiments by Kaushal and Tomita (2007) on fine glass-bead slurry

The calibration strategy was firstly applied to the flow conditions extracted from the experimental tests on fine glass-bead slurry flow performed by Kaushal and Tomita (2007). The experiments were performed in a pipe with a diameter of 54.9 mm using glass beads with density of 2470 kg/m^3 and mean particle diameter of 150 µm. The narrow particle size distribution enabled the assumption of mono-disperse particles, inherent to the two-fluid modelling approach. The ranges of average velocity and in-situ concentration considered in the present study were 2 to 5 m/s and 10 to 40 %, respectively, disregarding the data at $V_m = 1$ m/s and those at $C_{vi} = 50$ % because they were out of the range of applicability of the β-σ two-fluid model. For each condition, Kaushal and Tomita (2007) provided the hydraulic gradient and the concentration profile. In order to measure the latter quantity, they used a sampling probe and a γ-ray radiometric device, detecting full consistency of the two measurement techniques for fine glass beads. The concentration profiles obtained with the γ-ray device, which were the chord-average ones, were considered for comparison with the CFD simulations.

The first-attempt value of β was 0.5, and the case $V_m = 4$ m/s and $C_{vi} = 10$ % was chosen for the calibration of σ. As it is shown in **Fig. 7a**, the predicted concentration profile with $\sigma = 0.5$ was in very good agreement with the experimentally determined for this case, and additional tests confirmed the same finding for the other flow velocities with $C_{vi} = 10$ %. However, it must be observed that the

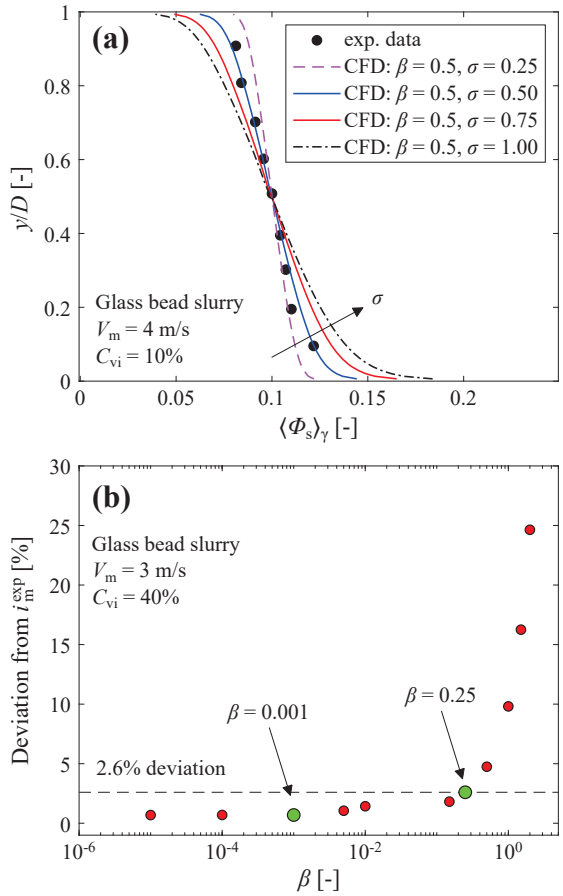

Fig. 7 Calibration for glass bead slurry (data from Kaushal and Tomita 2007): **(a)** calibration of σ based on the measured concentration profile for $V_m = 4$ m/s and $C_{vi} = 10$ % ($\beta = 0.25$); **(b)** calibration of β based on the measured hydraulic gradient for $V_m = 3$ m/s and $C_{vi} = 40$ % ($\sigma = 0.50$).

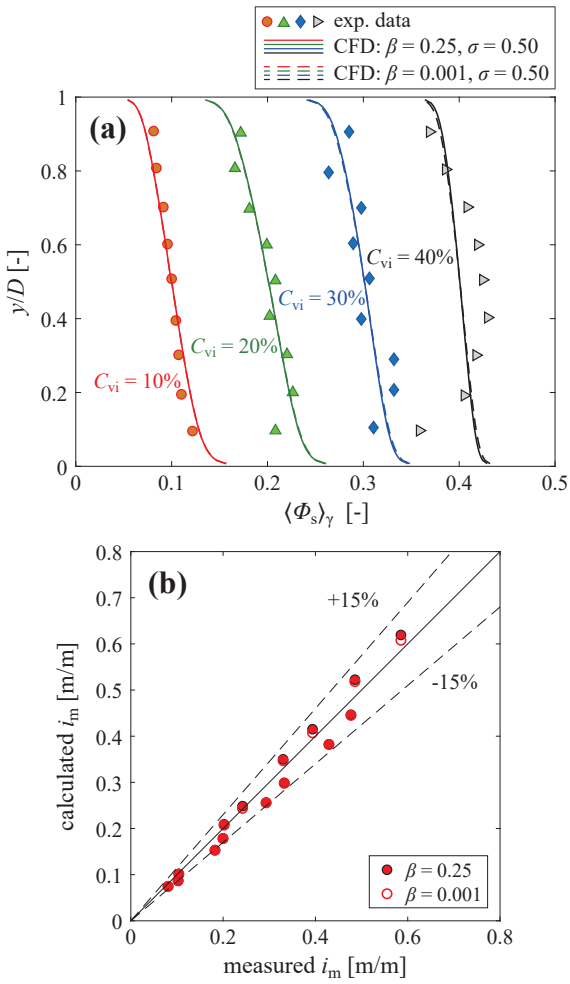

Fig. 8 Validation of the model with $\beta = 0.25$ and $\sigma = 0.5$ (continuous lines, filled points) and $\beta = 0.001$ and $\sigma = 0.5$ (dotted lines, unfilled points) for glass bead slurry (data from Kaushal and Tomita 2007): **(a)** concentration profiles for $V_m = 3$ m/s **(b)** hydraulic gradient.

uncertainty of the concentration data was not considered, as this information is difficult to estimate and it was not reported by the experimenters. Indeed, the consistency of the concentration profiles obtained by the sampling probe and the γ-ray device indicates the reliability of the data, but it is well known that local concentration values might be quite inaccurate close to the pipe bottom. This leads to the conclusion that it is not possible nor meaningful to seek for an "optimum" value for σ in a strict sense but, rather, the goal is to find "reasonably accurate" value of σ.

Once σ was defined as 0.5, an appropriate value of β was determined by referring to the measured hydraulic gradient for $V_m = 3$ m/s and $C_{vi} = 40$ %. **Fig. 7b** shows the percentage deviation between predicted and measured i_m for different values of β. The CFD model overestimates i_m for every β. Particularly, for β ranging from 10^{-5} to 0.25, the calculated hydraulic gradient is minorly affected by the value of β, both in absolute terms (i_m varies from 0.2437 m/m to 0.2483 m/m), as well as in terms of relative deviation from the experimental value (which is between 0.70 % and 2.60 %). The impossibility to find an "optimum" value of β which fully matches the experimentally-determined hydraulic gradient suggests that there exists some intrinsic limitation in the β-σ formulation, which prevents its ability to capture accurately the physical processes driving slurry flows at high concentration. Nonetheless, in this first test case, the accuracy of the β-σ two-fluid model in terms of hydraulic gradient is high (<2.60 %) for every β between 10^{-5} and 0.25. Considering that the simulation convergence was more and more difficult to achieve as β decreased, probably because of issues in the numerical evaluation of $\tilde{\mu}_m$ through Eqn. (5), initially it was decided to take $\beta = 0.25$. Such value did not produce any convergence issue, and resulted in a 2.6 % overestimation of the hydraulic gradient in the calibration case, which was judged a satisfactory enough level of agreement.

The conjecture underlying the proposed calibration strategy is that the pair of values $\sigma = 0.5$ and $\beta = 0.25$ allow for reasonably accurate prediction of concentration profile and hydraulic gradient for C_{vi} between 10 % to 40 % (that is, within the calibration conditions) and for V_m between 1.41 m/s and 5.95 m/s (as obtained from Eqns. (10) and (9), respectively). This could be partially verified through

validation with respect to all other testing conditions reported at the beginning of the present section (14 cases in total), for which however, the velocity range is a little bit narrower (2 m/s to 5 m/s).

With $\beta = 0.25$ and $\sigma = 0.5$, reasonable agreement was obtained in terms of the concentration profile, as exemplified through the continuous lines in **Fig. 8a** for $V_m = 3$ m/s and increasing C_{vi}. The β-σ two-fluid model is able to accurately predict the concentration profiles up to $C_{vi} = 30$ %. Conversely, for $C_{vi} = 40$ %, the experimental data suggested a reverse slope close to the pipe invert, and this effect is not captured by the CFD model, resulting in rather poorly predicted concentration profile. This give strength to the claim that there exists some inherent inability of the β-σ two-fluid model to capture the physics of highly concentrated slurry flows at high velocity, which cannot be remedied simply by adjusting β. Particularly, the absence of the lift force in generalized drag term could explain why the β-σ two-fluid model is not able to reproduce the reversal in the slope of the concentration profile observed experimentally, as already guessed by Kaushal et al. (2013). Additionally, it is not excluded that particle–particle collisions could take place for slurry flows at $C_{vi} = 40$ %, even at high flow velocity. The β-σ formulation is not able to account for these effects, which is instead a peculiar feature of two-fluid models based on the Kinetic Theory of Granular flow, such as those used by Ekambara et al. (2009) and Kaushal et al. (2013).

Beyond these considerations, the parity plot in **Fig. 8b** indicates the capacity of the β-σ two-fluid model with $\beta = 0.25$ and $\sigma = 0.5$ in predicting the hydraulic gradient with satisfactory accuracy (the filled points correspond to this combination of β and σ). The maximum absolute deviation between calculated and measured i_m is 17.5 %, and the mean absolute deviation is 8.70 %.

A weak point in the analysis here above relies in the choice of the value of $\beta = 0.25$, which appears quite arbitrary. As already noticed, the points in **Fig. 7b** indicate that every value of β within 10^{-5} and 0.25 produces broadly the same hydraulic gradient prediction, which is also close to the measured value (deviation < 2.60 %), but the numerical convergence becomes more and more difficult as β decreases. In order to investigate the actual impact of β on the predictive capacity of the β-σ two-fluid models, the simulations were repeated with $\beta = 0.001$ and $\sigma = 0.5$ and the new results are shown in **Fig. 8** using dotted lines and unfilled points. No differences are detected in terms of concentration profile. At first glance, this finding might appear in contrast with the results of the sensitivity analysis shown in **Fig. 4c**, indicating an influence of β on the concentration profile for case C6 in which $C_{vi} = 40$ %. However, the inconsistency might be explained considering that the two values of β compared in **Fig. 8a** (0.001 and 0.25) are lower than the range of β in the sensitivity analysis (0.5 to 3.5) and, additionally, that the horizontal axis is relatively narrow in **Fig. 4c**. Similar considerations can be made to explain why, in the parity plot in **Fig. 8b**, the effect of β on the predicted hydraulic gradient is very moderate, and visible only for a couple of points, whereas **Table 2** indicates a higher degree of influence for cases with $C_{vi} = 40$ % (C3, C4, C6). The comparison in **Fig. 8** indicates that even the impossibility to identify an "optimum" β does not affect the overall degree of accuracy of the β-σ model, thus its engineering effectiveness. It also gives strength to our claim that the poor agreement between measured and calculated concentration profiles at $C_{vi} = 40$ % is not a consequence of an inappropriate value of β, but, rather, is due to some intrinsic modelling limitation.

4.2 Experiments by Matoušek (2002) on fine sand slurry

A second verification of the calibration procedure was performed by referring to fine sand slurry flow experiments reported in Matoušek (2002), in which the pipe diameter is of 150 mm and the solids have a density of 2650 kg/m^3

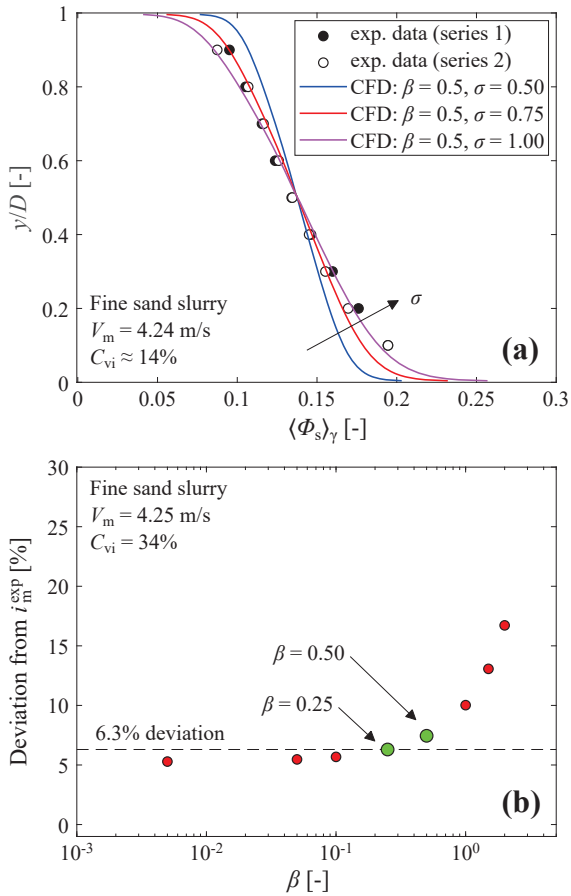

Fig. 9 Calibration for fine sand slurry (data from Matoušek 2002): **(a)** calibration of σ based on the measured concentration profile for $V_m = 4.24$ m/s and $C_{vi} = 14$ % ($\beta = 0.50$); **(b)** calibration of β based on the measured hydraulic gradient for $V_m = 4.25$ m/s and $C_{vi} = 34$ % ($\sigma = 0.75$). Both repetitions are shown in plot **(a)**, whether the mean hydraulic gradient between the two repetitions is considered in plot **(b)**.

and a mean particle diameter of 130 µm. Only six testing situations fulfill the applicability conditions of the β-σ two-fluid model, corresponding to two values of V_m (≈4.2 m/s and ≈6 m/s), and three levels of C_{vi} (≈14 %, ≈28 %, ≈33–34 %). For the six cases, the experimenter provided hydraulic gradient and chord-average concentration profiles by repeating the tests twice.

The concentration profile for $V_m = 4.24$ m/s and $C_{vi} \approx 14$ % was used to decide an appropriate σ, using a first-attempt β equal to 0.5. The findings in **Fig. 9a** indicate that a good match with the experimental data is obtained for $\sigma = 0.75$ and $\sigma = 1$, and the former value is used in the remaining simulations. Afterwards, a suitable value for β was determined from the measured hydraulic gradient for $V_m = 4.25$ m/s and $C_{vi} \approx 34$ %. The points in **Fig. 9b** show some similarity with the corresponding ones for fine glass-bead slurry, shown in **Fig. 7b**. In both cases, in fact, the calculated i_m increases with increasing β, and shows a plateau for low values of this coefficient. However, a difference exists in terms of the deviation between the predicted and the calculated i_m within the plateau region, which is around 0.7 %–2.6 % in the previous glass-bead case (**Fig. 7b**, in which $C_{vi} = 40$ %), and around 6 % for the present fine sand case (**Fig. 9b**, in which $C_{vi} = 34$ %). This indicates that, in the fine sand case, the inherent limitations in the β-σ formulation for highly concentrated slurries have an obvious impact on the accuracy of the hydraulic gradient predictions despite the lower value of C_{vi} (34 % instead of 40 %). As a first-attempt, it was decided to use the same value of β of the glass-bead case, that is, $\beta = 0.25$, which corresponds to an overestimation of the hydraulic gradient of about 6.3 %.

With $\beta = 0.25$ and $\sigma = 0.75$, the predicted concentration profile was in a good agreement with the experimental data in Matoušek (2002) for all the five conditions (note that the sixth profile had been already used for calibrating σ). Exemplary results are reported for $V_m \approx 6$ m/s in **Fig. 10a**, using continuous lines to denote the CFD predictions with $\beta = 0.25$ and $\sigma = 0.75$. In this second test case, the concentration profile is well predicted even for the highest value of C_{vi} (34 %), in contrast to the findings of the first validation example (grey-black series in **Fig. 8a**, where the C_{vi} was 40 %). This suggest that the limitations of the β-σ formulation affect different features of the CFD solution, depending on the testing conditions. In the first validation example, the hydraulic gradient was well predicted but the concentration profile was not. In the second test case, the situation seemed to be the opposite. The deviation in terms of hydraulic gradient prediction is within 15 % for five points out over six, and equal to 9.4 % on average (filled points in **Fig. 10b**). This indicates that the predictive capacity of the calibrated model can be satisfactory for the applications, although obviously a six-point population is not sufficient to provide accurate statistics.

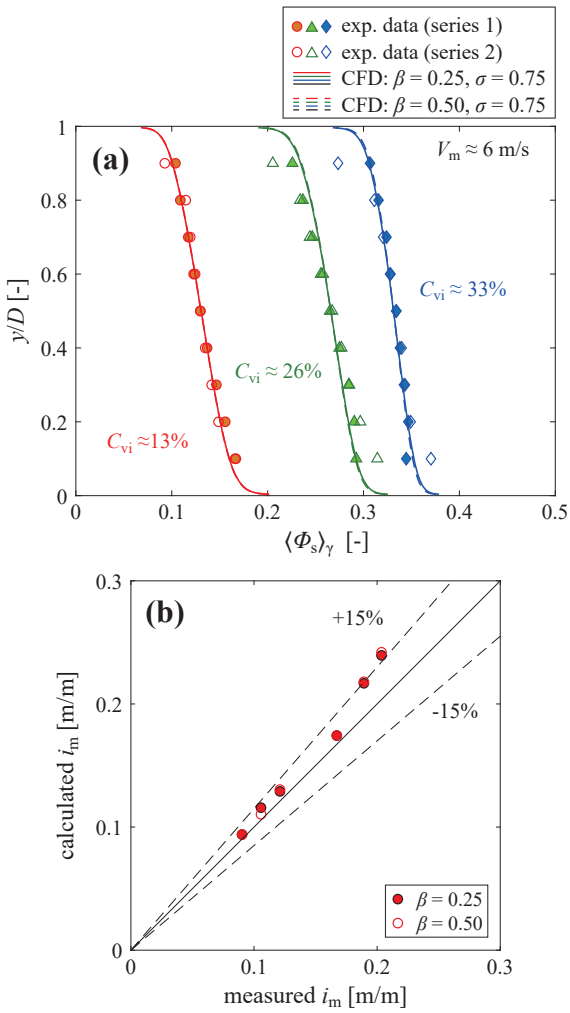

Fig. 10 Validation of the model with $\sigma = 0.75$ and $\beta = 0.25$ (continuous lines, filled points) and $\beta = 0.50$ (dotted lines, unfilled points) for fine sand slurry (data from Matoušek 2002): **(a)** concentration profiles (both repetitions are shown); **(b)** hydraulic gradient (experimental data are the average over the two repetitions).

As for the glass bead case, also in the fine sand one the first-attempt value of β is quite arbitrary, owing to the presence of a plateau in **Fig. 9b**. Thus, it was decided to investigate how the choice of a different value of β affects the predictive capacity of the model. The new value of β was 0.50, which, in **Fig. 9b**, is outside the plateau region and produces an overestimation of the hydraulic gradient of about 7.5 %. In **Fig. 10**, the CFD results obtained with $\beta = 0.50$ and $\sigma = 0.75$ are shown using dotted lines or unfilled points. Similarly to what has been obtained in **Section 4.1**, changing β did not produce appreciable variations in terms of the concentration profiles and, except for a couple of points, even for the hydraulic gradient. Once again, the lack of influence of β even for the highest concentration observed in **Fig. 9** is not inconsistent with the findings of the sensitivity analysis shown in **Table 2** and **Fig. 4**. In fact, this can be explained through a number of reasons, such as: (1) the two values of β in **Fig. 9** (0.25 and 0.50)

are quite close to each other and below the range used in the sensitivity analysis (0.5 to 3.5); (2) the horizontal axis in **Fig. 10a** is much more restricted than that in **Fig. 4c**; (3) the maximum C_{vi} in **Fig. 10**, equal to 34 %, is lower than the maximum C_{vi} in the sensitivity analysis, equal to 40 %.

4.3 Experiments by Schaan et al. (2000) on Lane Mountain sand slurry

In the final verification test, use was made of data reported in Schaan et al. (2000). Among the experiments described in the paper, calculations are directed to those performed in a 158.5 mm pipe using Lane Mountain sand. This type of sand is composed of small grains (median particle size is 90 µm) with high angularity, which produce significant frictional losses when flowing at high concentration. The density of the particles is the typical value for sand, that is 2655 kg/m^3. Hydraulic-gradient data and a few chord-averaged concentration profiles were provided for V_m between 1 m/s and 5 m/s and three levels of C_{vi} between about 14 % and about 39 %.

The case $V_m = 3$ m/s and $C_{vi} \approx 14$ % was considered for determining an appropriate value of σ by imposing the agreement between the calculated and the measured concentration profile. Based on the obtained results, shown in **Fig. 11a**, it was chosen to set σ equal to 0.75. Then, $V_m = 3$ m/s and $C_{vi} \approx 39$ % were used to decide on the β value. The relative deviation from the experimentally determined hydraulic gradient versus β, shown in **Fig. 11b**, suggests a similar trend to those of the two other test cases, if ones considers that the horizontal axis in **Fig. 11b** is not in log-scale and that the range of β was narrower. The tendency of the points towards some limiting deviation for lower β is evident, which confirms the modelling limitations of the β-σ formulation for high concentration. Nonetheless, here it was possible to identify a value of β (that is, 3.75) which fully matches the measured hydraulic gradient. Thus, the coefficients values $\sigma = 0.75$ and $\beta = 3.75$ were judged appropriate for Lane Mountain sand flow in a 150 mm pipe, with C_{vi} between 14 and 39 % (as obtained from the two calibration cases), and V_m between 1.79 m/s and 10 m/s (as obtained from Eqns. (10) and (9), respectively).

Validation was performed with respect to all other data reported in Schaan et al. (2000) fulfilling the conditions

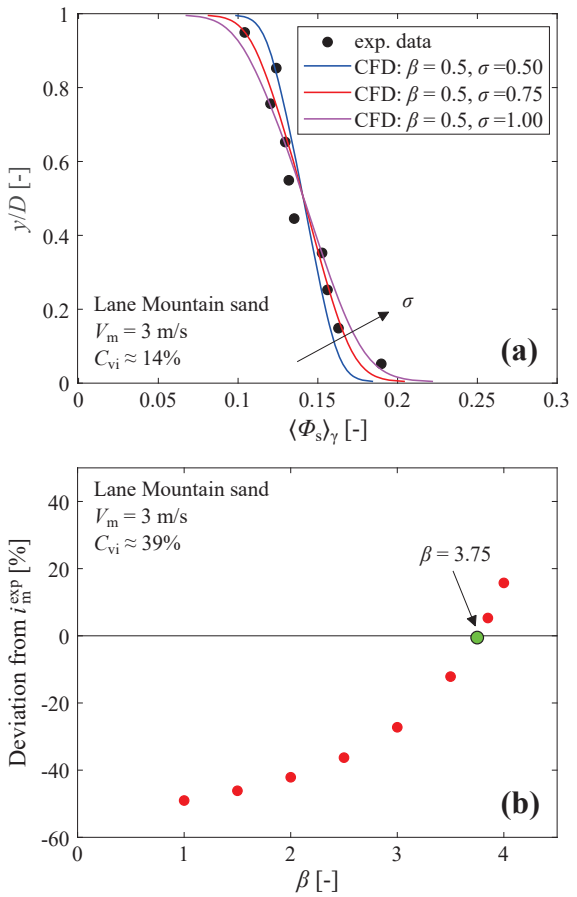

Fig. 11 Calibration for Lane Mountain sand slurry (data from Schaan et al. 2000): **(a)** calibration of σ based on the measured concentration profile for $V_m = 4.24$ m/s and $C_{vi} = 14$ %; **(b)** calibration of β based on the measured hydraulic gradient for $V_m = 3$ m/s and $C_{vi} = 40$ %.

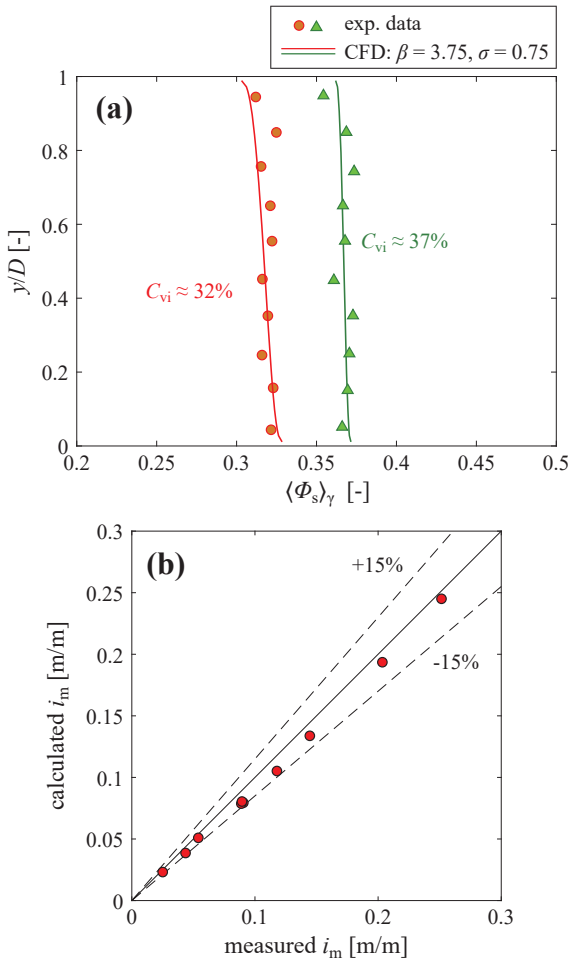

Fig. 12 Validation of the model with $\sigma = 0.75$ and $\beta = 3.75$ for Lane mountain sand (data from Schaan et al. 2000): **(a)** exemplary comparison of concentration profiles for $V_m = 3$ m/s; **(b)** parity plot of predicted vs measured hydraulic gradient.

above. The accuracy was satisfactory in terms of both concentration profiles and hydraulic gradient, as shown in **Fig. 12**.

As a final note, the value of β in the third validation example is significantly higher than that of the other two. This might be a consequence of the high angularity of the Lane Mountain sand particles used in the experiments of Schaan et al. (2000). This suggests that, as already guessed in one of the first papers concerning the β-σ two-fluid models (Messa and Malavasi, 2015), the parameter β might be related with the effect of particle shape. Nonetheless, a full understanding of the features of the slurry flows dictating the values of β and σ has not been achieved yet, and it will drive the future research efforts of the authors.

5. Conclusions and open questions

The present research work marked a step forward in the use of the β-σ two-fluid model as an engineering-effective tool with predictive capability. Particularly, the focus was on the analysis of the role played by the two main tuning coefficients of the model, namely, β and σ. The main findings are as follows:

- The value of σ mainly affects the slope of the predicted concentration profile, without any influence on the hydraulic gradient and on the velocity field. The value of β is important for slurries with high in-situ concentration and it affects both the hydraulic gradient and the solid concentration profile, but not the velocity field. The role played by β and σ on the different features of the CFD solution does not depend on flow velocity and pipe diameter.
- A procedure has been proposed for deciding the values of β and σ through experimental calibration. It consists firstly in evaluating σ based on a single concentration profile at low in-situ concentration (say around 10 %), followed by the calculation of an appropriate β based on a single hydraulic gradient point at high slurry concentration (say around 30–40 %). This strategy relies on the negligible effect of β on the solution of the β-σ two-fluid model at low slurry concentration.
- The calibration procedure was verified based on experimental data reported in the literature, referring to both glass bead and sand slurry. The validation study indicated some degree of robustness of the calibrated parameters with respect to changes in velocity, particle size, and in-situ concentration. It has also been shown that, although in some cases it might not be possible to find a value of β which fully matches the measured hydraulic gradient for the high concentration calibration case, selecting different values of β within a reasonable range does not affect the overall performance of the β-σ two-fluid model. The level of accuracy appears generally satisfactory for the application requirements but it might result in poor predictions for highly concentrated slurries (in-situ concentration higher than about 35 %).

At the same time, some unresolved issues demand for further research. Two examples are given below.

Firstly, the calibration yielded for $\sigma = 0.50$ and $\sigma = 0.75$ intended for the validation tests on glass beads and the two types of sand, respectively. Bearing in mind that no optimum value of σ could be obtained in a strict sense, due to the uncertainty of the local volume fraction measurements, in order to provide a better characterization of σ it would be important to understand the origin of this difference. Is it due to the different material (glass beads versus sand) and/or to the different pipe size (54.9 mm versus 150 mm)? Or do other factors come into play? Similar open questions can be made for β, which appears related with the shape of the particles, but still lacks of a comprehensive characterization.

Additionally, the data in **Figs. 7b**, **9b** and **11b**, indicate that, for highly concentrated slurries, the hydraulic gradient is insensitive to β below a certain threshold. This is a limitation of the β-σ formulation, which appears uncapable of reproducing all the physical mechanisms driving the transport of massive amounts of particles, thus demanding for further improvement. At the moment, the impact of this limitation varies according to the specific testing conditions. In the first two validation examples (glass bead slurry and fine sand slurry), it led to the already mentioned impossibility of finding an optimum β which matches the experimentally determined hydraulic gradient. Indeed, such limiting deviation is more significant for the fine sand case (≈6 %, **Fig. 9b**) rather than for the glass bead one (<2.6 %, **Fig. 7b**), where, however, inaccuracies are observed in terms of the concentration profile (**Fig. 8a**, grey-black series). In the last validation example, which refers to slurry with highly angular particles, a best value of β was identified (**Fig. 11b**) and, based on the available data, the predictions are accurate in terms of both concentration profile and hydraulic gradient (**Fig. 12**).

Acknowledgements

The research at University of Coimbra was sponsored by national funds through FCT—Fundação para a Ciência e a Tecnologia, under projects UIDB/00102/2020 and UIDB/00285/2020.

Data Availability Statement

The data analysis file and the data supporting the findings of this study are available in J-STAGE Data (https://doi.org/10.50931/data.kona.19861708).

References

Burns A.D., Frank T., Hamill I., Shi J.-M., The Favre averaged drag model for turbulent dispersion in Eulerian multi-phase flows, in: Proceedings of the 5th International Conference on Multiphase Flow (ICMF-2004), Yokohama, Japan, May

30–June 4, 2004.

Capecelatro J., Desjardins O., Eulerian–Lagrangian modeling of turbulent liquid–solid slurries in horizontal pipes, International Journal of Multiphase Flow, 55 (2013) 64–79. DOI: 10.1016/j.ijmultiphaseflow.2013.04.006

CHAM (Concentration, Heat and Momentum Limited), The PHOENICS encyclopaedia, Two-phase flows, 1994a, <www.cham.co.uk/phoenics/d_polis/d_lecs/ipsa/ipsa.htm> accessed 24.03.2022.

CHAM (Concentration, Heat and Momentum Limited), The PHOENICS encyclopaedia, Turbulence models for two-phase flows, 1994b, <www.cham.co.uk/phoenics/d_polis/d_enc/turmod/enc_tu7.htm> accessed 24.03.2022.

CHAM (Concentration, Heat and Momentum Limited), The PHOENICS encyclopaedia, Equilibrium log-law wall functions, 1994c, <www.cham.co.uk/phoenics/d_polis/d_enc/turmod/enc_tu8.htm> accessed 24.03.2022.

CHAM (Concentration, Heat and Momentum Limited), PHOENICS Overview: CHAM Technical Report TR001, 2002, <www.cham.co.uk/phoenics/d_polis/d_docs/tr001/tr001.htm> accessed 24.03.2022.

Cheng N.-S., Law A.W.-K., Exponential formula for computing effective viscosity, Powder Technology, 129 (2003) 156–160. DOI: 10.1016/S0032-5910(02)00274-7

Durand R., Basic relationships o the transportation of solids in pipes – experimental research, in: Proceedings of the 5th IAHR Congress, Minneapolis, Minnesota, USA, 1–5 September 1953.

Ekambara K., Sanders R.S., Nandakumar K., Masliyah J.H., Hydrodynamic simulation of horizontal slurry pipeline flow using ANSYS-CFX, Industrial & Engineering Chemistry Research, 48 (2009) 8159–8171. DOI: 10.1021/ie801505z

Kaushal D.R., Thinglas T., Tomita Y., Kuchii S., Tsukamoto H., CFD modeling for pipeline flow of fine particles at high concentration, International Journal of Multiphase Flow, 43 (2012) 85–100. DOI: 10.1016/j.ijmultiphaseflow.2012.03.005

Kaushal D.R., Tomita Y., Experimental investigation for near-wall lift of coarser particles in slurry pipeline using γ-ray densitometer, Powder Technology, 172 (2007) 177–187. DOI: 10.1016/j.powtec.2006.11.020

Launder B.E., Spalding D.B., The numerical computation of turbulent flows, Computer Methods in Applied Mechanics and Engineering, 3 (1974) 269–289. DOI: 10.1016/0045-7825(74)90029-2

Ling J., Skudarnov P.V., Lin C.X., Ebadian M.A., Numerical investigations of liquid–solid slurry flows in a fully developed turbulent flow region, International Journal of Heat and Fluid Flow, 24 (2003) 389–398. DOI: 10.1016/S0142-727X(03)00018-3

Matoušek V., Krupička J., Konfršt J., Pěník V., Internal structure of settling-slurry flows: solids distribution and friction in horizontal pipe, in: Proceedings of the 16th International Conference on Transport and Sedimentation of Solid Particles, Rostock, Germany, 18–20 September 2013.

Matousek V., Pressure drops and flow patterns in sand-mixture pipes, Experimental Thermal and Fluid Science, 26 (2002) 693–702. DOI: 10.1016/S0894-1777(02)00176-0

Messa G.V., Malin M., Malavasi S., Numerical prediction of fully-suspended slurry flow in horizontal pipes, Powder Technology, 256 (2014) 61–70. DOI: 10.1016/j.powtec.2014.02.005

Messa G.V., Malin M., Matoušek V., Parametric study of the β-σ two-fluid model for simulating fully suspended slurry flow: effect of flow conditions, Meccanica, 56 (2021a) 1047–1077. DOI: 10.1007/s11012-021-01314-6

Messa G.V., Malavasi S., Improvements in the numerical prediction of fully-suspended slurry flow in horizontal pipes, Powder Technology, 270 (2015) 358–367. DOI: 10.1016/j.powtec.2014.10.027

Messa G.V., Matoušek V., Analysis and discussion of two fluid modelling of pipe flow of fully suspended slurry, Powder Technology, 360 (2020) 747–768. DOI: 10.1016/j.powtec.2019.09.017

Messa G.V., Yang Q., Adedeji O.E., Chára Z., Duarte C.A.R., Matoušek V., Rasteiro M.G., Sanders R.S., Silva R.C., de Souza F.J., Computational fluid dynamics modelling of liquid–solid slurry flows in pipelines: state-of-the-art and future perspectives, Processes, 9 (2021b) 1566. DOI: 10.3390/pr9091566

Roco M.C., Shook C.A., Modeling of slurry flow: the effect of particle size, The Canadian Journal of Chemical Engineering, 61 (1983) 494–503. DOI: 10.1002/cjce.5450610402

Schaan J., Sumner R.J., Gillies R.G., Shook C.A., The effect of particle shape on pipeline friction for Newtonian slurries of fine particles, The Canadian Journal of Chemical Engineering, 78 (2000) 717–725. DOI: 10.1002/cjce.5450780414

Schiller L., Naumann A., A drag coefficient correlation, Zeitschrift des Vereins Deutscher Ingenieure, 77 (1935) 318–320.

Schlichting H., Boundary-Layer Theory, 7th ed., McGraw-Hill, New York, 1979, ISBN: 9780070553347.

Thomas A.D., Predicting the deposit velocity for horizontal turbulent pipe flow of slurries, International Journal of Multiphase Flow, 5 (1979) 113–129. DOI: 10.1016/0301-9322(79)90040-5

Thomas A., A modification of the Wilson & Judge deposit velocity equation, extending its applicability to finer particles and larger pipe sizes, in: Proceedings of the 17th Conference on Transport and Sedimentation of Solid Particles, Delft, The Netherlands, 22–25 September 2015.

Uzi A., Levy A., Flow characteristics of coarse particles in horizontal hydraulic conveying, Powder Technology, 326 (2018) 302–321. DOI: 10.1016/j.powtec.2017.11.067

Wilson K.C., A unified physically based analysis of solid-liquid pipeline flow, in: Proceedings of the 4th International Conference on Hydrotransport, Banff, Canada, 18–21 May 1976.

Wilson K.C., Addie G.R., Sellgren A. Clift R., Slurry Transport Using Centrifugal Pumps, 3rd ed., Springer, New York, , 2006, ISBN: 9780387232621.

Authors' Short Biographies

Gianandrea Vittorio Messa

Gianandrea Vittorio Messa studied Civil Engineering (Hydraulics) at Politecnico di Milano, where he received the M.Sc. cum laude and the PhD with honors in 2009 and 2013, respectively. Since 2021, he is Associate Professor at Politecnico di Milano, where he teaches courses of Fluid Mechanics and Hydraulics. His main research interest is the numerical modelling of particle-laden flows and related phenomena, such as slurry pipe transport and slurry erosion of pipeline components.

Qi Yang

Qi Yang is currently a Ph.D. candidate in Civil and Environmental engineering at Politecnico di Milano. His doctoral work is focused on the CFD modelling of slurry flow in pipelines, including development and application of Eulerian-Eulerian two-fluids models.

Maria da Graça Rasteiro

Maria da Graça Rasteiro graduated in Chemical Engineering at the University of Coimbra, did post graduate studies in Loughborough University, UK, and obtained a PhD in Chemical Engineering/Multiphase Processes, in 1988, at the University of Coimbra, under the co-supervision of Professor Brian Scarlett. She is presently an Associate Professor with Aggregation in the Chemical Engineering Department of the University of Coimbra in Portugal. She is a member of the working groups on Particle Characterization and Particle Mechanics of the European Federation of Chemical Engineering, and is presently a member of the Portuguese Engineers Association and a founding member of the Portuguese Society for Engineering Education (SPEE). Her research interests have always been in the field of Particle Technology and she started the first Portuguese laboratory on particle characterization. Presently, she has got research interests in the field of particle aggregation, development of natural polymers for particle flocculation including microplastics, rheology of particle suspensions, solid/liquid flow modelling including fiber flow modelling, and on experimental techniques for flow visualization including tomographic techniques.

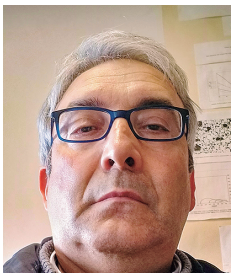

Pedro M. Faia

Pedro M. Faia received his degree in Electrical Engineering (1990), his M.S. in Automation (1994) and his Ph.D in Electronic Materials (2003) from the University of Coimbra. He is an Auxiliary Professor at the Department of Electrical Engineering and Computers of the University of Coimbra where he teaches. His research interest's concern: chemical and electrochemical sensors; impedance spectroscopy technique and applications; electric and ionic materials characterization; Electrical Impedance Tomography for multiphase flow visualization; Instrumentation.

Václav Matoušek

Václav Matoušek is Full Professor of Water Engineering and Water Management at Faculty of Civil Engineering of Czech Technical University in Prague. He received the Master Degree in Civil Engineering at this university in 1986 and the PhD in Mechanical (Dredging) Engineering from the Delft University of Technology, the Netherlands, in 1997. His research focuses primarily on two-phase flows with a special attention to pipeline transport of slurries, slurry pumping, rheology of mixtures, flow of rheologically active slurries, sediment transport in open channels and river morphology.

Authors' Short Biographies

Rui César Silva

Rui César Silva has a background in chemical engineering from the University of Porto and in 2016 attained his PhD approval from the University of Coimbra, under the theme Solid-liquid suspension flow in pipes: modelling and experimental investigation where the first Portuguese electrical tomography system was successfully constructed. He worked at Hovione Farmaciência, a pharmaceutical CDMO, from 2016 until 2021, acting as technical scientific leader on several projects with topics ranging from particle engineering, hollow-fiber separations, chemical process modelling and data science. During his tenure at this company, he was one of fastest members to achieved seniority and lead projects to commercialization, through process performance qualification, in record time. He authored several works presented at scientific conferences and served as a tutor on both Master and PhD thesis on hollow-fiber crystallization and particle size reduction technologies. Presently, he works in R&D Process Development and Scale-up at Amyris Portugal.

Fernando A. P. Garcia

Fernando A. P. Garcia was graduated as a chemical engineer in the Instituto Superior Técnico of the Technical University of Lisbon. He obtained a Master degree in Biological Engineering in Chemical Engineering and then a PhD degree in Chemical Engineering in the University of Birmingham, UK. He started his academic career in the University of Coimbra, first as an assistant demonstrator in the areas of fluid dynamics and transport phenomena. After his doctorate he became an Assistant Professor and later an Associate Professor. Apart from the transport phenomena, his main interests are in the area of biocatalysis and downstream operations of fermentation processes and in treatment of industrial effluents. He is a member of several scientific institutions. He served as secretary of the ESAB, the European Section of Applied Biocatalysis of the European Federation of Biotechnology and later as a member of the Executive Board.